Computational study of hippocampal-septal theta rhythm changes due to Beta-amyloid-altered ionic channels

OPEN ACCESS Freely available online

PLoS one

Computational Study of Hippocampal-Septal Theta Rhythm Changes Due to Beta-Amyloid-Altered Ionic Channels

Xin Zou*, Damien Coyle, KongFatt Wong-Lin, Liam Maguire

Intelligent Systems Research Centre, University of Ulster Magee Campus, Derry, Northern Ireland, United Kingdom

Abstract

Electroencephagraphy (EEG) of many dementia patients has been characterized by an increase in low frequency field potential oscillations. One of the characteristics of early stage Alzheimer's disease (AD) is an increase in theta band power (4–7 Hz). However, the mechanism(s) underlying the changes in theta oscillations are still unclear. To address this issue, we investigate the theta band power changes associated with β-Amyloid (Aβ) peptide (one of the main markers of AD) using a computational model, and by mediating the toxicity of hippocampal pyramidal neurons. We use an established biophysical hippocampal CA1-medial septum network model to evaluate four ionic channels in pyramidal neurons, which were demonstrated to be affected by Aβ. They are the L-type Ca^{2+} channel, delayed rectifying K^+ channel, A-type fast-inactivating K^+ channel and large-conductance Ca^{2+}-activated K^+ channel. Our simulation results demonstrate that only the Aβ inhibited A-type fast-inactivating K^+ channel can induce an increase in hippocampo-septal theta band power, while the other channels do not affect theta rhythm. We further deduce that this increased theta band power is due to enhanced synchrony of the pyramidal neurons. Our research may elucidate potential biomarkers and therapeutics for AD. Further investigation will be helpful for better understanding of AD-induced theta rhythm abnormalities and associated cognitive deficits.

Citation: Zou X, Coyle D, Wong-Lin K, Maguire L (2011) Computational Study of Hippocampal-Septal Theta Rhythm Changes Due to Beta-Amyloid-Altered Ionic Channels. PLoS ONE 6(6): e21579. doi:10.1371/journal.pone.0021579

Editor: Stephen D. Ginsberg, Nathan Kline Institute and New York University School of Medicine, United States of America

Received March 9, 2011; **Accepted** June 2, 2011; **Published** June 24, 2011

Funding: This study is currently supported under the CNRT award by the Northern Ireland Department for Employment and Learning through its "Strengthening the All-Island Research Base" initiative. The funders had no role in study design, data collection and analysis, decision to publish, or preparation of the manuscript.

Competing Interests: The authors have declared that no competing interests exist.

* E-mail: x.zou@ulster.ac.uk

Introduction

Alzheimer's disease (AD) is a neurodegenerative disease associated with memory deficits and cognitive decline, which may be induced by anatomical and physiological changes in the brain. AD is characterized by two neuropathological structures: neurofibrillary tangles and senile plaques. The neurofibrillary tangles are the residue of neuronal death, which may be caused by the microtubule-binding protein, tau, becoming hyperphosphorylated. The senile plaques are mainly composed of Aβ. Aβ acts as a neurotoxin causing neuronal dysfunction and apoptosis [1]. As Aβ precedes tau protein in AD progress [2], we will focus on Aβ in this work.

It has also been found that pathological changes in the brain can lead to abnormalities in oscillations of field potentials recorded by EEG [3,4,5] and local field potential (LFP) [6]. The AD induced brain field potentials oscillation abnormalities and the cause of these abnormalities are complex. Previous studies have shown that early stages of AD are characterized by an increase in theta band (4–7 Hz) power and decrease in beta band (13–30 Hz) and alpha band (8–12 Hz) power [3,7,8]. The abnormalities may be caused by the pathological changes in many brain regions, e.g., medial temporal lobe and cortex [9]. In this work, we will focus on the Aβ affected hippocampal pyramidal neurons and the associated theta band power changes for various reasons, e.g., the hippocampus is affected at the early onset of AD [10], especially the pyramidal cells in the hippocampus [4] and the hippocampus and the associated medial septum are one of the major sources of low frequency theta oscillation.

Aβ (mainly $Aβ_{1-42}$) can oligomerize and permeate into the cell membrane, which can break down the regulation of Ca^{2+} movement and ionic homeostasis of neurons [11]. Aβ may change the activity of various ionic channels, e.g., Aβ has been found to be able to potentiate L-type Ca^{2+} channels [12,13]. Aβ also affects K^+ channels, which have an intimate relationship with the cell resting potential and membrane repolarization. It has been reported in [14] that low concentration of Aβ blocks A-type fast-inactivating K^+ channels and a high concentration of Aβ can also block delayed rectifying K^+ channels. The effect of Aβ on large-conductance Ca^{2+}-activated K^+ channels (BK) is still a subject of debate. BK channels were reported to be activated by Aβ [15,16,17]. However, other research has shown that Aβ suppresses BK channels in some cases [18,19,20]. Arispe et al. [21] proposed a hypothesis that Aβ could also form new cation channels in neuronal membrane. In addition, Aβ can disturb the neurotransmitter systems by inducing cholinergic and glutamatergic dysfunctions [22]. All of the pathological changes outlined above may result in alterations in theta band power. As a first step in our study, we focus on the changes in these four ionic channels, i.e., L-type Ca^{2+} channel (I_{Ca}); A-type fast-inactivating K^+ channel (I_A), delayed rectifying K^+ channel (I_K) and large-conductance Ca^{2+}-activated K^+ channel (I_{CT}), and evaluate any corresponding change in hippocampal theta band power.

To investigate the effect of Aβ on hippocampo-septal theta rhythm, we make use of a biophysical model of the hippocampal CA1 region and the medial septum. The spiking neuronal network model consists of hippocampal principle pyramidal neurons, basket and OLM interneurons and the medial septal MSGABA neurons. The model of pyramidal neurons is constructed based on [23,24]. The basket, OLM and MSGABA interneurons are modelled in the same way as presented in [25,26]. Synapses in our work are mediated by typical neurotransmitters $GABA_A$, NMDA and AMPA, which are based on [27]. The aim is to evaluate the relationship between Aβ induced changes in ionic channels (I_{Ca}, I_K, I_A and I_{CT}) and the theta band power alterations. The effects of Aβ on those channels are simulated by changing the amplitudes of these ionic currents. Our simulation results show that theta band power is highly dependent on I_A but not I_{Ca}, I_K and I_{CT}. In particular, theta band power significantly increases with a decrease in I_A. We propose that this increased theta band power is induced by the enhanced synchrony of pyramidal neurons. This hypothesis is supported by our simulation results.

Methods

We construct a network model of hippocampus CA1-medial septum based on the Hodgkin-Huxley type formalisms presented in [27]. The model incorporates three types of neurons from the hippocampus, i.e., excitatory pyramidal, inhibitory basket and OLM neurons and inhibitory MSGABA neurons from the medial septum. These neurons have been demonstrated to contribute to theta rhythm activity in *in vivo* experiments [28,29,30] and in simulation studies [26,31]. A schematic diagram of the neuronal network architecture is illustrated in Figure 1. Each type of neuron in Figure 1 represents a population of identical neurons.

The pyramidal neurons are modelled by a two-compartmental model, one for the soma and the other for the dendrite. As in [23], the soma compartment has spike generating currents I_{Na} and I_K and the dendrite contains a calcium dependent potassium current I_{AHP}. Both the soma and dendrite contain leakage currents I_L and high-threshold L-type calcium currents I_{Ca} plus hyperpolarization-activated currents I_h. The pyramidal neurons in hippocampus CA1 contain additional ionic currents to account for different neuronal functions [24]. In this work, we select some of these currents, which have been shown to be affected by Aβ. As a result, our model also contains an A-type potassium current I_A and a large-conductance calcium dependent potassium current I_{CT} in the soma and dendrite, respectively. The Hodgkin-Huxley type dynamical equations for the pyramidal neurons are:

$$\frac{dV_s}{dt} = -I_L - I_{Na} - I_K - I_{Ca} - I_A - I_{CT} - I_h - \frac{g_c}{p}(V_s - V_d) - I_{syn,s} + I \quad (1)$$

$$\frac{dV_d}{dt} = -I_L - I_{Ca} - I_{AHP} - I_A - I_{CT} - I_h - \frac{g_c}{1-p}(V_d - V_s) - I_{syn,d} \quad (2)$$

where subscript s and d denotes soma and dendrite, respectively. I is the injected DC current and I_{syn} is the synaptic currents from interneurons.

The other three inhibitory neurons are modelled as one-compartment. The model of basket neurons has I_{Na}, I_K, and leakage current I_L, Eq. 3. The model of OLM has I_{Na}, I_K, I_L, I_{Ca}, hyperpolarization activated current I_h and I_{AHP}, Eq. 4. MSGABA contains I_{Na}, I_K, I_L and a slowly inactivating potassium current I_{KS}, Eq. 5.

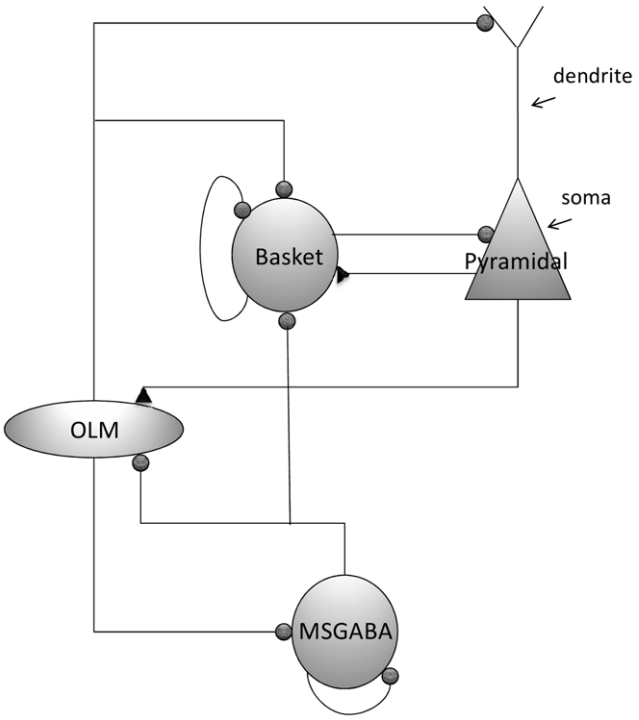

Figure 1. Hippocampo-septal network architecture. The network consists of four types of neuronal populations, i.e., pyramidal, basket, OLM and MSGABA neurons. Inhibitory $GABA_A$-mediated synaptic connections are indicated by '●', and excitatory AMPA and NMDA-mediated synaptic connections are indicated by '▲'.
doi:10.1371/journal.pone.0021579.g001

$$\text{Basket}: \frac{dV}{dt} = -I_L - I_{Na} - I_K - I_{syn} + I \quad (3)$$

$$\text{OLM}: \frac{dV}{dt} = -I_L - I_{Na} - I_K - I_{Ca} - I_h - I_{AHP} - I_{syn} + I \quad (4)$$

$$\text{MSGABA}: \frac{dV}{dt} = -I_L - I_{Na} - I_K - I_{KS} - I_{syn} + I \quad (5)$$

To emulate heterogeneity in the real brain tissues, the injected DC current I for each neuron is not chosen to be identical. This is done by allowing I to follow a Gaussian distribution with mean I_μ and standard derivation I_σ. I_μ for the pyramidal, basket, OLM and MSGABA neuronal populations are chosen to be $5\mu A/cm^2$, $1.4\mu A/cm^2$, $0\mu A/cm^2$ and $2.2\mu A/cm^2$, respectively. As there is no agreement on the specific I_σ to be used, we chose $I_\sigma = 0.1\mu A/cm^2$ for all populations for simplicity. This heterogeneity will be implemented in all our simulations. Definitions of all the other parameters are given in Appendix S1.

The number of pyramidal, basket, OLM and MSGABA neurons are 10, 100, 30 and 50, respectively [27]. In the network, the pyramidal neurons innervate basket neurons via neurotransmitter AMPA and OLM via AMPA+NMDA, other synaptic connections are mediated by $GABA_A$ neurotransmitter. We model their effects with rise and decay time constants of their synaptic

gating variables. It has been shown in [32] that the synaptic time constants have the equivalent effect of the conduction delays on the postsynaptic activities. Slight changes in these time contents do not affect our conclusion. The network is constructed using a sparse connectivity i.e., the neurons are randomly coupled with a fixed average number of pre-synaptic inputs/post-synaptic outputs per neuron. The number of pre-synaptic inputs/post-synaptic outputs is adjusted according to [27].

We compute the LFP signal as a sum of the values of the synaptic currents of the pyramidal neurons [33]. This is under the assumption that pyramidal neurons contribute more to the overall signal due to their approximate open field arrangement. The fast components of the LFP are reduced by low pass filtering (0–40 Hz). The power spectrum is obtained by a fast Fourier transform with a 2 s length Hanning window. The relative theta band power (% of the total power) is calculated. A membrane potential noise that follows a Gaussian distribution with zero mean and *1.5mV* standard derivation is also introduced in some of the following simulations. The membrane noise is randomly generated in each trial that lasts for 10 s. Each presented result is obtained from simulations averaged over 15 trials of the model representing different individual patients. We found that higher number of trials does not alter the obtained average theta band power. The results from trials of the model run with normal parameter settings are considered as a "healthy" control group whereas trials with alterations to parameters of various ionic channels simulate deficiencies and are considered as potential different "patient" groups. Various ionic channels are potentiated or suppressed to simulate the effects of Aβ, which will be presented in the next section. All of the results were obtained by adjusting the ionic currents in the pyramidal neurons only. The statistical significance of the differences between groups is evaluated using a one-way ANOVA test. Error bars are standard errors.

Results

The dynamics of neurons in theta oscillation obtained in control condition are demonstrated in Figure 2. To better illustrate the spiking phases of different neuronal populations, membrane noise is removed. Figure 2 shows that theta oscillation is generated by the spiking of different neuronal populations clustered at certain phases. Assuming a network theta oscillation begins with spikes from the pyramidal neurons. Then the OLM neurons are evoked via the excitatory synaptic connections from the pyramidal neurons, which produce a feedback inhibition to the pyramidal neurons. The basket neurons then gradually depolarize and produce series of spikes. The spikes of basket neurons are inhibited by the spiking of MSGABA neurons. The slowly inactivating potassium current I_{KS} in MSGABA neuron plays a very important role in the theta generation, which is referred to as a 'pacemaker' for theta rhythm [26].

It has been pointed out that the main cause of the loss of intracellular calcium homeostasis in AD patients is that Aβ can potentiate the L-type Ca^{2+} channels (I_{Ca}) [13], which causes a large influx of Ca^{2+} into the cells. The mechanism of Aβ increasing the influx of Ca^{2+} is still unclear. Aβ may form new cation channels and/or alter the existing L-type Ca^{2+} channels. In our simulations, we emulate the effect of Aβ by increasing the maximum conductance of the L-type Ca^{2+} channels. The obtained theta band power with enhanced I_{Ca} is presented in Figure 3. It can be seen that changes in L-type Ca^{2+} channels do not cause a change in theta rhythm.

Aβ also blocks some K^+ ionic channels in pyramidal neurons, e.g., I_A and I_K [14,34]. The experimental results showed that Aβ is more likely to block the channel from outside the neurons. Therefore we emulate the effect of Aβ by decreasing the maximum conductance of I_A and I_K, respectively. Furthermore, it has been shown that I_A has larger density in dendrite compared with soma [35] and Aβ have much greater effect on the dendrite I_A [36,37]. Based on these findings, only I_A in the dendrite will be reduced. The simulation results obtained in control and decreased I_A in the dendrite only conditions are illustrated in Figure 4. Our simulation shows that theta band power is significantly increased ($p<0.05$) as I_A decreases. An example of the auto-correlation of the summation of all membrane potentials and the corresponding band power in control and $0.6g_A$ conditions is illustrated in Figure 5 and 6. It can be seen that theta oscillation and its power is significantly increased with low g_A. Similar changes in theta band power due to I_K (via g_K) are not observed, as illustrated in Figure 7.

As AD disturbs the homeostasis of Ca^{2+}, the Ca^{2+}-activited BK channel (I_{CT}) is vulnerable to AD pathology. BK channel can adjust the spike broadening during repetitive firing [38] and spiking frequency [39]. Previous research reveals that the activity of BK channel is probably promoted by Aβ [17]. However, other research reports that BK channel is suppressed in some cases [18,19,20]. Therefore, we have simulated both increased and blocked I_{CT} in our simulations. I_{CT} is potentiated by increasing the fraction of Ca^{2+} influx, B (see Appendix S1). The simulation results are illustrated in Figure 8. It can be seen that neither blockage nor potentiation in I_{CT} can affect theta rhythm.

The simulation results have shown that a decrease in I_A can significantly increase theta band power. To evaluate whether this is due to an enhanced synchrony of neuronal populations, we calculate the population coherence coefficient [40]. In this section, g_A is decreased in both soma and dendrite simultaneously. The long time interval T ($T=2s$ in our experiment) is first divided into small bins of $\tau=1ms$ and spike trains of the i^{th} and j^{th} neurons in the population are given $X_i(l), X_j(l)=1$or 0, $l=1,...,K(K=T/\tau)$, where '*1*' denotes spiking and '*0*' resting. The coherence coefficient κ_{ij} between the trains can be calculated as

$$\kappa_{ij}=\frac{\sum_{l=1}^{K} X_i(l)X_j(l)}{\sqrt{\sum_{l=1}^{K} X_i(l)\sum_{l=1}^{K} X_j(l)}} \quad (6)$$

The whole populationκ is obtained by averaging all of the combinations of i and j. κ is calculated for the control group and the group with decreased g_A. In the following simulations, I_A in both soma and dendrite are decreased simultaneously. The obtained κ is illustrated in Figure 9. Consistent with our hypothesis, population synchrony is significantly increased as g_A decreases ($p<0.001$).

The increased synchrony is probably caused by the enhanced excitability and firing rate of the pyramidal neurons. To support this hypothesis, the firing rates of the pyramidal neuronal population with various values of g_A are shown in Figure 10. It can be clearly seen that the decreased g_A has enhanced the excitability of the pyramidal neurons and their firing rates. Therefore, we suggest that when I_A is decreased, the pyramidal neurons become more excitable. During the peak of each pyramidal population theta cycle, more pyramidal neurons spike simultaneously, which enhances the synchrony of the population.

In summary, our simulations have shown that a decrease in I_A in the pyramidal neurons induces an increase in theta band power by recruiting more pyramidal neurons to fire.

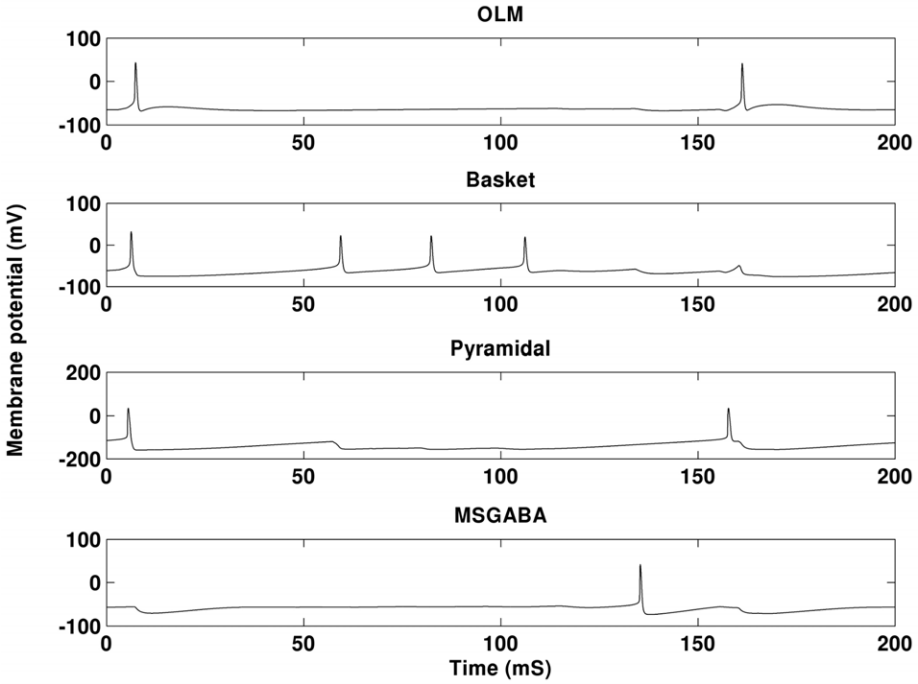

Figure 2. Membrane potential dynamics in theta oscillation. Each individual network theta oscillation period consists of spikes of different neuronal populations clustering around different phases. The figures are obtained in control condition without membrane noise.
doi:10.1371/journal.pone.0021579.g002

Discussion

AD is usually accompanied with alterations in neuronal network oscillations. The patterns of oscillation changes in different frequency bands have been used to discriminate the AD-induced dementia from the other dementias [41]. The aim of our work is to better understand the mechanisms underlying these oscillation abnormalities. We have investigated rhythms using other types of models and looked at connectivity changes in our previous work, e.g., we have investigated the AD-induced alpha rhythm abnormalities [42] and the relationship between changes in alpha and theta rhythms [43] using an abstract model. In this work, we

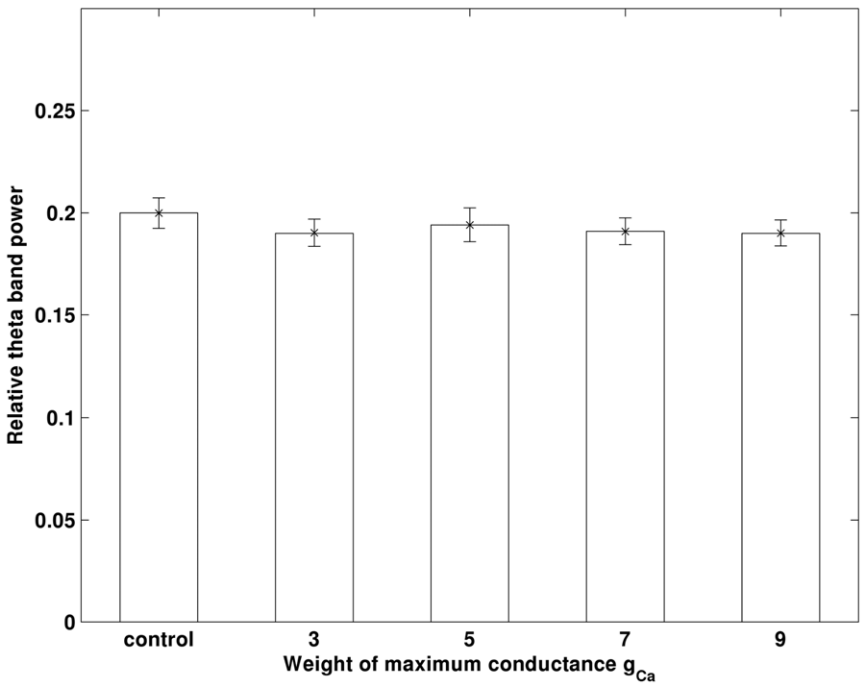

Figure 3. Increase in g_{Ca} does not induce changes in theta band power. In the figure, the obtained average theta band power of each experiment is illustrated. Errorbar is standard error.
doi:10.1371/journal.pone.0021579.g003

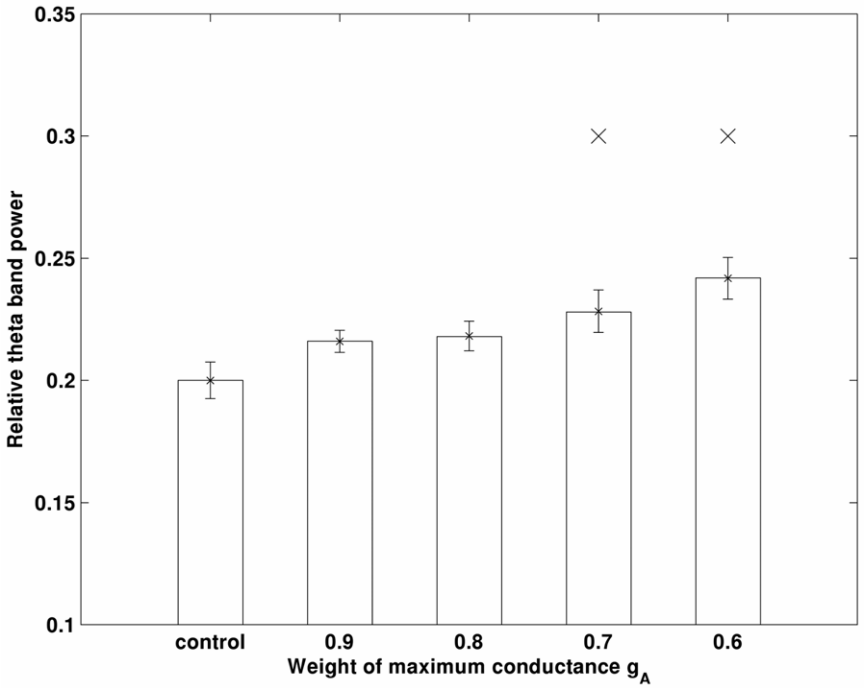

Figure 4. Theta band power increases with decrease in g_A. × indicates that power is significantly larger than that obtained in control condition ($p<0.05$). Errorbar is standard error.
doi:10.1371/journal.pone.0021579.g004

investigated the Aβ-induced theta oscillation abnormality based on a conductance-based hippocampo-septal model.

Previous experimental results have demonstrated that Aβ can induce neuronal dysfunction by altering certain ionic channels. The computational simulations have shown that some of the ionic channels play critical roles in the neuronal network oscillations, e.g., [26]. However, the mechanisms underlying Aβ induced hippocampo-septal theta rhythm alteration remains unclear. In this work, the change in theta band power caused by Aβ has been investigated using a conductance-based hippocampus CA1 and

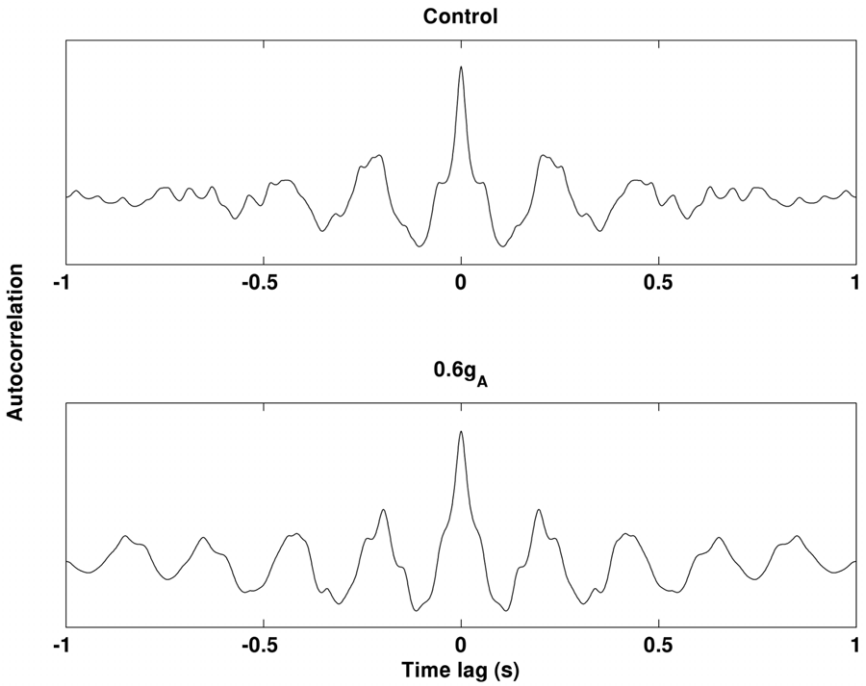

Figure 5. The auto-correlations of a summation of membrane potentials obtained in control and $0.6g_A$ conditions. Theta rhythm is strengthened by decreased g_A. Both of the results are obtained in the same noisy and heterogenous condition obtained in single trial.
doi:10.1371/journal.pone.0021579.g005

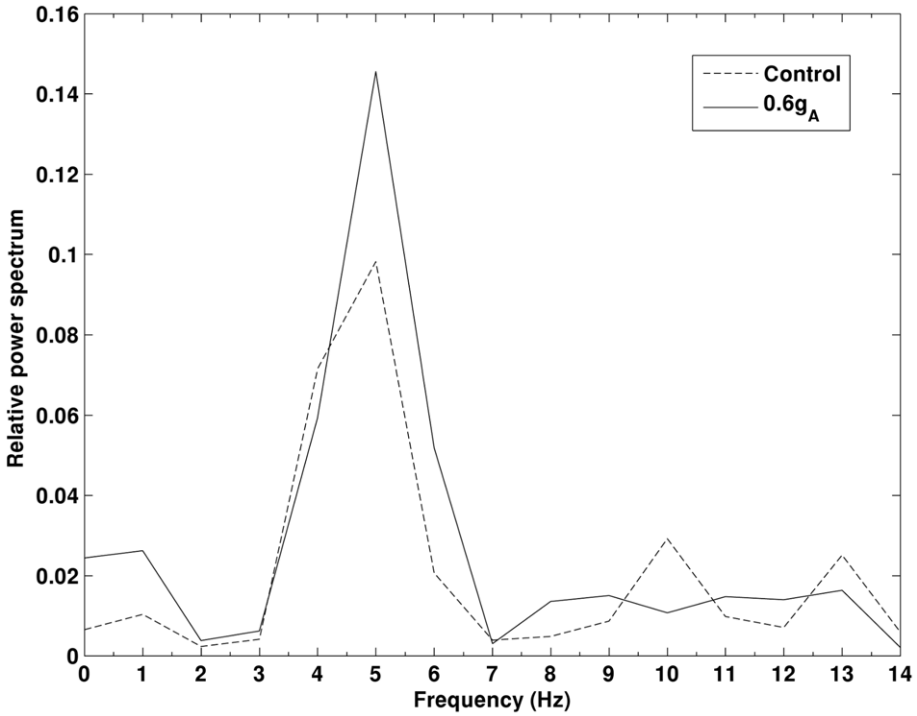

Figure 6. More significant power spectrum peak in theta band in $0.6g_A$ condition than in control condition. Both of the results are obtained in the same noisy and heterogenous condition obtained in single trial.
doi:10.1371/journal.pone.0021579.g006

medial septum network model. Based on previous experimental results, the effect of Aβ was emulated by blocking or potentiating specific ionic channels. Then the corresponding theta band power was calculated and compared with that obtained in a control (normal) condition. We have evaluated four types of ionic channels, one Ca^{2+} and three K^+ channels. We have identified

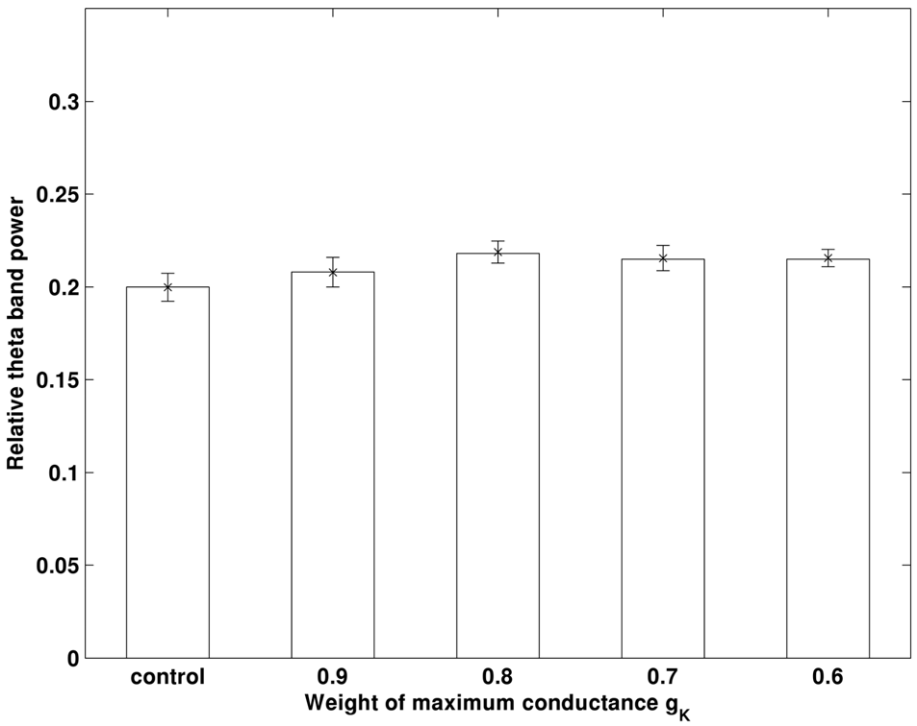

Figure 7. Decrease in g_K does not induce significant changes in theta band power. Errorbar is standard error.
doi:10.1371/journal.pone.0021579.g007

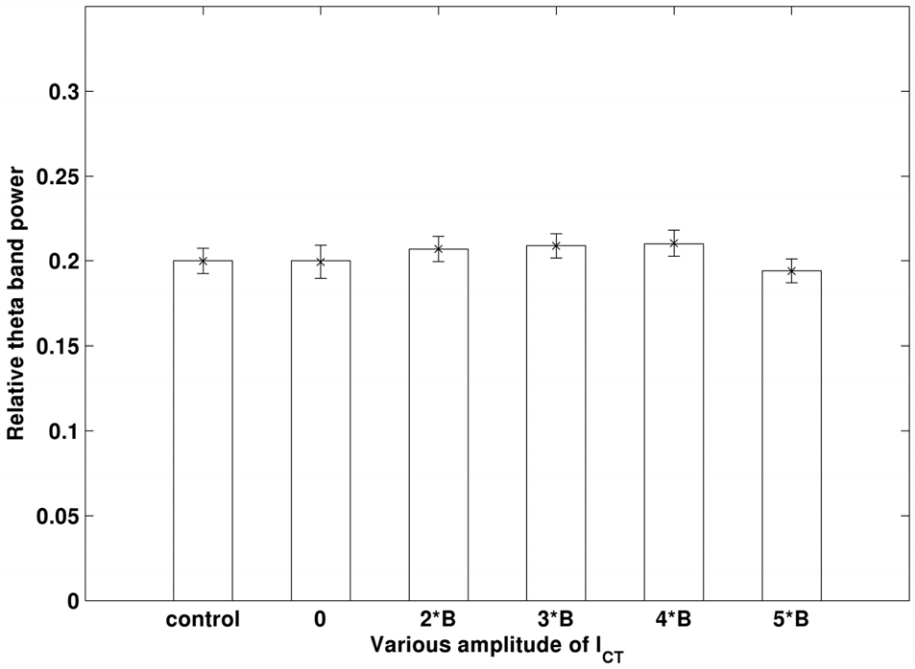

Figure 8. Change in I_{CT} does not induce significant changes in theta band power. Both the completely blocked I_{CT} (0) and the potentiated I_{CT} (2B, 3B, 4B, 5B) are evaluated. Errorbar is standard error.
doi:10.1371/journal.pone.0021579.g008

that only a decrease in fast-inactivating K^+ currents (I_A) affected theta band power. To explain its mechanism, we have proposed that the blockage of I_A by Aβ increases the excitability of pyramidal neurons, which led to more synchrony of pyramidal neuronal firings. The synchronized firing state then propagated to other neuronal populations. As a result, theta band power was increased. Our hypothesis has been supported by various simulations. Our computational work has shown that Aβ-induced

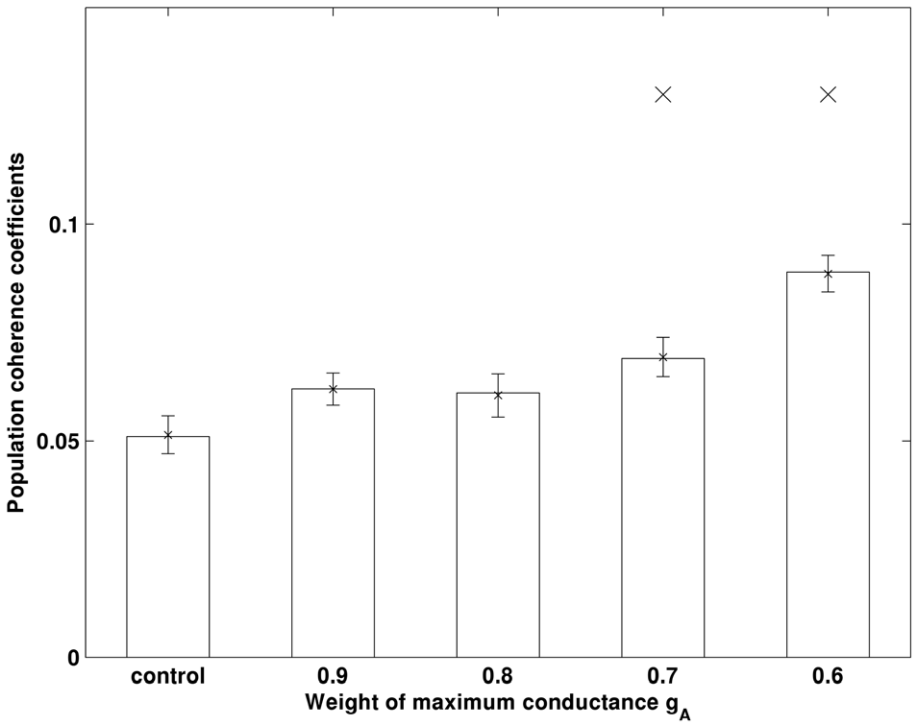

Figure 9. The pyramidal neuronal population coherence coefficients increase with g_A decreases. '×' indicates the coherence coefficient is significantly larger than that obtained in control condition ($p<0.01$). Errorbar is standard error.
doi:10.1371/journal.pone.0021579.g009

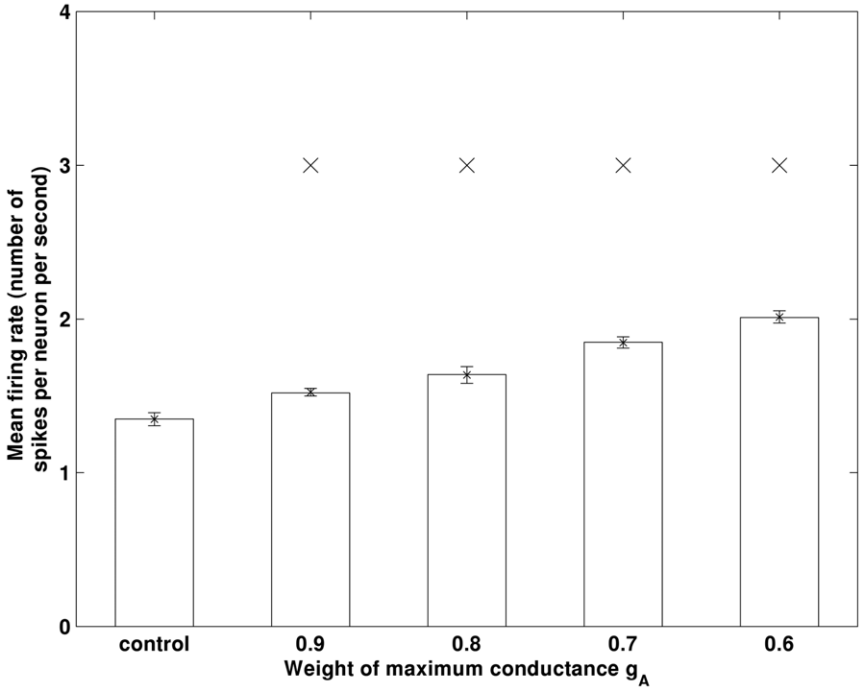

Figure 10. The pyramidal neuronal population firing rates increase with decrease in g_A. '×' indicates the firing rate is significantly larger than that obtained in control condition ($p<0.001$). Errorbar is standard error.
doi:10.1371/journal.pone.0021579.g010

I_A depression could be an important factor in causing theta rhythm abnormalities in AD. Our results may have implications for the development of the AD biomarkers and therapeutics. For example, drugs which can potentiate I_A may be used to counteract the affect of Aβ. In fact, cannabinoids which can potentiate I_A [44], have been successfully used in AD treatment [45].

In this work, we have observed that decreased I_A can enhance the excitability of the pyramidal neurons and result in higher theta band power. However, how alterations in I_A change the excitability of pyramidal neurons is still unclear. If the activation of I_A is long lasting, then the mechanism may be straightforward, as reducing a long lasting current may allow more neurons to spike

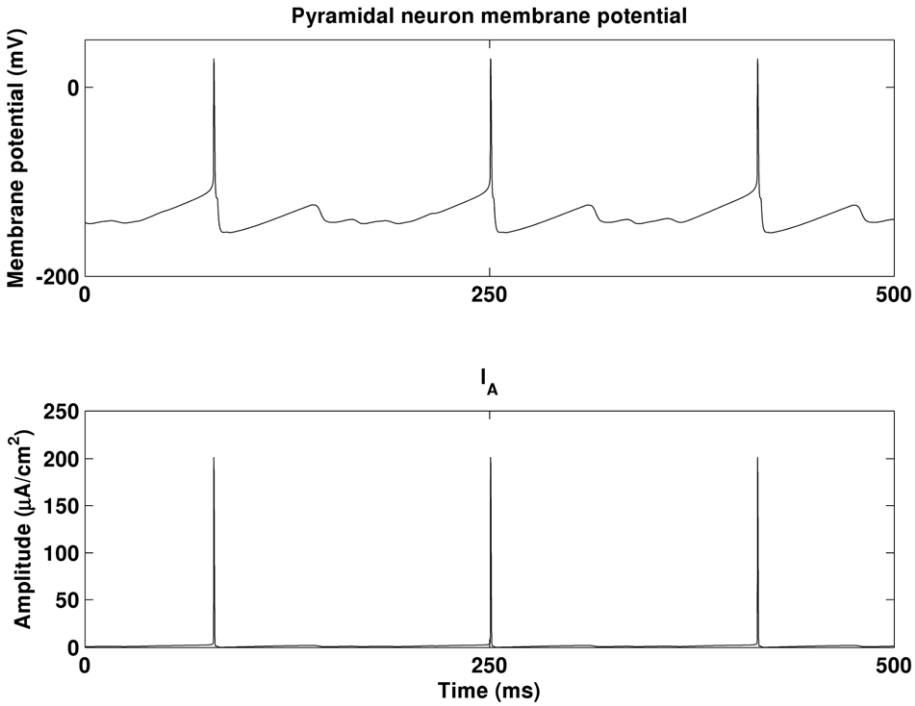

Figure 11. An example of dynamics of a pyramidal neurons and the associated brief transient I_A.
doi:10.1371/journal.pone.0021579.g011

per theta cycle. Figure 11 illustrates an example of dynamics of a pyramidal neuron and associated I_A. As shown, I_A actually operates very briefly as compared to theta rhythm. It resets shortly after a spike. Therefore, the mechanism underlying I_A-induced firing rate changes is a topic which deserves further attention and is the focus of our on-going research. Furthermore, we recognize that not all experimental observations fit with this picture of enhanced theta band power. For example, in [46], theta band power was found to decrease in rats' hippocampus injected with Aβ. The mechanism underlying Aβ induced theta band power decrease is also currently being investigated.

The long term potentiation and depression of synapses in the hippocampus play critical roles in the formation and processing of memories. Previous research [27] has shown that synaptic changes can also induce alterations in theta band power. To achieve this, the afference from other parts of brain, e.g., acetylcholine neuromodulation from medial septum, may be incorporated into the model. Furthermore, it has been found that AD is usually associated with an increase chance of unprovoked epilepsy [47]. In a recent study [48], it has been shown that Aβ could be the main cause of epilepsy in AD due to hippocampal network hyper-excitability. Our work could provide a potential explanation for this observation. We will address these issues in our future work.

Supporting Information

Appendix S1 Definition of the model parameters.
(DOC)

Acknowledgments

We are grateful to Dr. Tamas Kiss for help in the model construction.

Author Contributions

Conceived and designed the experiments: XZ DC KW LM. Performed the experiments: XZ DC KW. Analyzed the data: XZ DC KW. Contributed reagents/materials/analysis tools: XZ DC KW. Wrote the paper: XZ DC KW LM.

References

1. Hardy JA, Higgins GA (1992) Alzheimer's disease: the amyloid cascade hypothesis. Science 256: 184–185.
2. Takahashi RH, Capetillo-Zarate E, Lin MT, Milner TA, Gouras GK (2010) Co-occurrence of Alzheimer's disease ss-amyloid and tau pathologies at synapses. Neurobiol Aging 31: 1145–1152.
3. Ponomareva NV, Korovaitseva GI, Rogaev EI (2008) EEG alterations in non-demented individuals related to apolipoprotein E genotype and to risk of Alzheimer disease. Neurobiol Aging 29: 819–827.
4. Adeli H, Ghosh-Dastidar S, Dadmehr N (2005) Alzheimer's disease and models of computation: imaging, classification, and neural models. J Alzheimers Dis : -7: 187–199; discussion 255-162.
5. Dauwels J, Vialatte F, Cichocki A (2010) Diagnosis of Alzheimer's disease from EEG signals: where are we standing? Curr Alzheimer Res 7: 487–505.
6. Robbe D, Buzsaki G (2009) Alteration of theta timescale dynamics of hippocampal place cells by a cannabinoid is associated with memory impairment. J Neurosci 29: 12597–12605.
7. Ihl R, Dierks T, Martin EM, Froolich L, Maurer K (1996) Topography of the maximum of the amplitude of EEG frequency bands in dementia of the Alzheimer type. Biol Psychiatry 39: 319–325.
8. Chiaramonti R, Muscas GC, Paganini M, Muller TJ, Fallgatter AJ, et al. (1997) Correlations of topographical EEG features with clinical severity in mild and moderate dementia of Alzheimer type. Neuropsychobiology 36: 153–158.
9. Braak H, Braak E, Bohl J, Bratzke H (1998) Evolution of Alzheimer's disease related cortical lesions. J Neural Transm Suppl 54: 97–106.
10. Li X, Coyle D, Maguire L, Watson DR, McGinnity TM (2010) Gray matter concentration and effective connectivity changes in Alzheimer's disease: a longitudinal structural MRI study. Neuroradiology.
11. Shirwany NA, Payette D, Xie J, Guo Q (2007) The amyloid beta ion channel hypothesis of Alzheimer's disease. Neuropsychiatr Dis Treat 3: 597–612.
12. Davidson RM, Shajenko L, Donta TS (1994) Amyloid beta-peptide (A beta P) potentiates a nimodipine-sensitive L-type barium conductance in N1E-115 neuroblastoma cells. Brain Res 643: 324–327.
13. Webster NJ, Ramsden M, Boyle JP, Pearson HA, Peers C (2006) Amyloid peptides mediate hypoxic increase of L-type Ca2+ channels in central neurones. Neurobiol Aging 27: 439–445.
14. Good TA, Smith DO, Murphy RM (1996) Beta-amyloid peptide blocks the fast-inactivating K+ current in rat hippocampal neurons. Biophys J 70: 296–304.
15. Furukawa K, Barger SW, Blalock EM, Mattson MP (1996) Activation of K+ channels and suppression of neuronal activity by secreted beta-amyloid-precursor protein. Nature 379: 74–78.
16. Yu SP, Farhangrazi ZS, Ying HS, Yeh CH, Choi DW (1998) Enhancement of outward potassium current may participate in beta-amyloid peptide-induced cortical neuronal death. Neurobiol Dis 5: 81–88.
17. Ye H, Jalini S, Mylvaganam S, Carlen P (2010) Activation of large-conductance Ca(2+)-activated K(+) channels depresses basal synaptic transmission in the hippocampal CA1 area in APP (swe/ind) TgCRND8 mice. Neurobiol Aging 31: 591–604.
18. Qi JS, Qiao JT (2001) Suppression of large conductance Ca2+-activated K+ channels by amyloid beta-protein fragment 31-35 in membrane patches excised from hippocampal neurons. Sheng Li Xue Bao 53: 198–204.
19. Jhamandas JH, Cho C, Jassar B, Harris K, MacTavish D, et al. (2001) Cellular mechanisms for amyloid beta-protein activation of rat cholinergic basal forebrain neurons. J Neurophysiol 86: 1312–1320.
20. Chi S, Qi Z (2006) Regulatory effect of sulphatides on BKCa channels. Br J Pharmacol 149: 1031–1038.
21. Arispe N, Pollard HB, Rojas E (1993) Giant multilevel cation channels formed by Alzheimer disease amyloid beta-protein [A beta P-(1-40)] in bilayer membranes. Proc Natl Acad Sci U S A 90: 10573–10577.
22. Tran MH, Yamada K, Nabeshima T (2002) Amyloid beta-peptide induces cholinergic dysfunction and cognitive deficits: a minireview. Peptides 23: 1271–1283.
23. Wang X-J (1998) Calcium coding and adaptive temporal computation in cortical pyramidal neurons. J Neurophysiol 79: 1549–1566.
24. Warman EN, Durand DM, Yuen GL (1994) Reconstruction of hippocampal CA1 pyramidal cell electrophysiology by computer simulation. J Neurophysiol 71: 2033–2045.
25. Wang X-J, Buzsaki G (1996) Gamma oscillation by synaptic inhibition in a hippocampal interneuronal network model. J Neurosci 16: 6402–6413.
26. Wang X-J (2002) Pacemaker neurons for the theta rhythm and their synchronization in the septohippocampal reciprocal loop. Neurophysiology 87: 889–900.
27. Hajós M, Hoffmann WE, Orbán G, Kiss T, Érdi P (2004) Modulation of septo-hippocampal Theta activity by GABAA receptors: an experimental and computational approach. Neuroscience 126: 599–610.
28. Csicsvari J, Hirase H, Czurko A, Mamiya A, Buzsaki G (1999) Oscillatory coupling of hippocampal pyramidal cells and interneurons in the behaving Rat. J Neurosci 19: 274–287.
29. Ylinen A, Soltesz I, Bragin A, Penttonen M, Sik A, et al. (1995) Intracellular correlates of hippocampal theta rhythm in identified pyramidal cells, granule cells, and basket cells. Hippocampus 5: 78–90.
30. Klausberger T, Magill PJ, Marton LF, Roberts JD, Cobden PM, et al. (2003) Brain-state- and cell-type-specific firing of hippocampal interneurons in vivo. Nature 421: 844–848.
31. Rotstein HG, Pervouchine DD, Acker CD, Gillies MJ, White JA, et al. (2005) Slow and fast inhibition and an H-current interact to create a theta rhythm in a model of CA1 interneuron network. J Neurophysiol 94: 1509–1518.
32. Roxin A, Montbrio E (2010) How effective delays shape oscillatory dynamics in neuronal networks. Physica D: Nonlinear Phenomena 240: 323–345.
33. Mazzoni A, Whittingstall K, Brunel N, Logothetis NK, Panzeri S (2010) Understanding the relationships between spike rate and delta/gamma frequency bands of LFPs and EEGs using a local cortical network model. Neuroimage 52: 956–972.
34. Qi JS, Ye L, Qiao JT (2004) Amyloid beta-protein fragment 31-35 suppresses delayed rectifying potassium channels in membrane patches excised from hippocampal neurons in rats. Synapse 51: 165–172.
35. Hoffman DA, Magee JC, Colbert CM, Johnston D (1997) K+ channel regulation of signal propagation in dendrites of hippocampal pyramidal neurons. Nature 387: 869–875.
36. Chen C (2005) beta-Amyloid increases dendritic Ca2+ influx by inhibiting the A-type K+ current in hippocampal CA1 pyramidal neurons. Biochem Biophys Res Commun 338: 1913–1919.
37. Morse TM, Carnevale NT, Mutalik PG, Migliore M, Shepherd GM (2010) Abnormal Excitability of Oblique Dendrites Implicated in Early Alzheimer's: A Computational Study. Front Neural Circuits 4.
38. Shao LR, Halvorsrud R, Borg-Graham L, Storm JF (1999) The role of BK-type Ca2+-dependent K+ channels in spike broadening during repetitive firing in rat hippocampal pyramidal cells. J Physiol 521(Pt 1): 135–146.
39. Lancaster B, Nicoll RA (1987) Properties of two calcium-activated hyperpolarizations in rat hippocampal neurones. J Physiol 389: 187–203.
40. Gerstein GL, Kiang NY (1960) An approach to the quantitative analysis of electrophysiological data from single neurons. Biophys J 1: 15–28.

41. Bonanni L, Thomas A, Tiraboschi P, Perfetti B, Varanese S, et al. (2008) EEG comparisons in early Alzheimer's disease, dementia with Lewy bodies and Parkinson's disease with dementia patients with a 2-year follow-up. Brain 131: 690–705.
42. Bhattacharya B, Colye D, Maguire L (2011) A thalamo-cortico-thalamic neural mass model to study alpha rhythms in Alzheimer's Disease. (in press) Neural Networks Sp issue on Brain Disorders.
43. Bhattacharya B, Colyle D, Maguire L (2011) Alpha and theta rhythm abnormality in Alzheimer's Disease: a study using a computational model. (in press) in From Brains to Systems: Brain-Inspired Cognitive Systems 2010 (Eds) C Hernández, J Gómez, R Sanz, I Alexander, L Smith, A Hussain, A Chella, Series: Advances in Experimental Medicine and Biology, Springer New York 718.
44. Deadwyler SA, Hampson RE, Mu J, Whyte A, Childers S (1995) Cannabinoids modulate voltage sensitive potassium A-current in hippocampal neurons via a cAMP-dependent process. J Pharmacol Exp Ther 273: 734–743.
45. Volicer L, Stelly M, Morris J, McLaughlin J, Volicer BJ (1997) Effects of dronabinol on anorexia and disturbed behavior in patients with Alzheimer's disease. Int J Geriatr Psychiatry 12: 913–919.
46. Villette V, Poindessous-Jazat F, Simon A, Lena C, Roullot E, et al. (2010) Decreased rhythmic GABAergic septal activity and memory-associated theta oscillations after hippocampal amyloid-beta pathology in the rat. J Neurosci 30: 10991–11003.
47. Amatniek JC, Hauser WA, DelCastillo-Castaneda C, Jacobs DM, Marder K, et al. (2006) Incidence and predictors of seizures in patients with Alzheimer's disease. Epilepsia 47: 867–872.
48. Palop JJ, Chin J, Roberson ED, Wang J, Thwin MT, et al. (2007) Aberrant excitatory neuronal activity and compensatory remodeling of inhibitory hippocampal circuits in mouse models of Alzheimer's disease. Neuron 55: 697–711.